

Reconsideration of surface tension and phase state effects on CCN activity based on the AFM measurement~~Insights into the role of dicarboxylic acid on CCN activity: implications for surface tension and phase state effects~~

Chun Xiong¹, Xueyan Chen³, ~~Binyu Kuang¹~~, Xiaolei Ding^{4,3}, Binyu Kuang¹, Xiangyu Pei¹, Zhengning Xu¹, Shikuan Yang³, Huan Hu^{4,3*}, Zhibin Wang^{1,2,5,4*}

¹College of Environmental and Resource Sciences, Zhejiang University, Zhejiang Provincial Key Laboratory of Organic Pollution Process and Control, Hangzhou, China

²ZJU-Hangzhou Global Scientific and Technological Innovation Center, Hangzhou, China

³Institute for Composites Science Innovation, School of Materials Science and Engineering, Zhejiang University, Hangzhou, Zhejiang 310027, China

⁴Zhejiang University-University of Illinois at Urbana-Champaign Institute, International Campus, Zhejiang University, Haining 314400, China

⁵Key Laboratory of Environment Remediation and Ecological Health, Ministry of Education, Zhejiang University, Hangzhou, China

Correspondence to: Zhibin Wang (wangzhibin@zju.edu.cn~~wangzhibin@zju.edu.cn~~) and Huan Hu (huanhu@intl.zju.edu.cn~~huanhu@intl.zju.edu.cn~~)

Abstract. Dicarboxylic acids are ubiquitous in atmospheric aerosol particles, but their roles as surfactants in cloud condensation nuclei (CCN) activity remain unclear. In this study, we investigated CCN activity of inorganic salt (sodium chloride and ammonium sulfate) and dicarboxylic acid (including malonic acid (MA), phenylmalonic acid (PhMA), succinic acid (SA), phenylsuccinic acid (PhSA), adipic acid (AA), pimelic acid (PA) and octanedioic acid (OA)) mixed particles with varied organic volume fraction (OVF), and then directly determined their surface tension and phase state at high relative humidity (over 99.5%) by atomic force microscopy (AFM). Our results showed that CCN derived κ_{CCN} of studied dicarboxylic acids ranged in 0.003-0.240. A linearly positive ~~correlation~~relation between κ_{CCN} and solubility was obtained for slightly dissolved species, while negative ~~correlation~~relation was found between κ_{CCN} and molecular volume for highly soluble species. For most inorganic salt/dicarboxylic acid (MA, PhMA, SA, PhSA and PA), a good closure within 30% relative bias between κ_{CCN} and chemistry derived κ_{Chem} ~~were~~was obtained. However, κ_{CCN} values of inorganic salt/AA and inorganic salt/OA systems were surprisingly 0.3-3.0 times higher than κ_{Chem} , which was attributed to surface tension reduction as AFM results showed that their surface tensions were 20%-42% lower than that of water (72 mN m⁻¹). Meanwhile, semisolid phase states were obtained for inorganic salt/AA and inorganic salt/OA and ~~may~~also affected hygroscopicity closure results. Our study highlights that surface tension reduction should be considered to investigate aerosol-cloud interactions.

32 1 Introduction

33 Atmospheric particles can indirectly affect global climate through their impacts on aerosol-cloud interaction by serving as
34 cloud condensation nuclei (CCN) (Rosenfeld et al., 2014). Exploring the factors affecting CCN activation ~~could~~ can help to
35 understand the aerosol-cloud interactions and thus decrease the uncertainty in the assessment of climate model. Köhler theory
36 provides the basis for linking CCN activity with aerosol thermodynamic properties (Köhler, 1936), in which size and chemical
37 composition are key factors to determine the activation of aerosol particles. Previous studies pointed out that aerosol number
38 size distribution ~~is~~ was essential to determine CCN concentration other than composition (Dusek et al., 2006; Gunthe et al.,
39 2009; Rose et al., 2010). The role of particle chemistry in the activation process, however, is still debatable due to the
40 complexity of chemical constitution. ~~(Bhattu and Tripathi, 2015; Noziere, 2016).~~

41 Single parameter κ was introduced in Köhler theory to describe hygroscopicity of aerosol particles (Petters and Kreidenweis,
42 2007). κ -Köhler theory usually performed well in predictions of hygroscopicity and CCN number concentration (Rose et al.,
43 2010; Kawana et al., 2016; Cai et al., 2020; Zhang et al., 2020). However, remarkable offset was also found because of the
44 simplifications in κ -Köhler theory (Ruehl et al., 2016; Ovadnevaite et al., 2017). For example, aerosol droplet is assumed to
45 be diluted near activation and surface tension is usually simply treated as that of pure water, which is sometimes not reasonable
46 in the presence of atmospheric surfactants (Lowe et al., 2019). ~~Yet m~~ Many previous studies investigated surface tension effect
47 of atmospheric surfactant on aerosol CCN activity (Ruehl and Wilson, 2014; Ruehl et al., 2016; Ovadnevaite et al., 2017). At
48 Mace Head, Ovadnevaite et al. (2017) observed significant underestimation of CCN number concentration (one tenth) in a
49 nascent ultrafine mode event with high organic mass fraction (55%). The underestimation was improved by applying lower
50 water surface tension ($\sim 68\%$ of water surface tension). For surfactant sodium octyl sulfate, Peng et al. (2022) found that CCN-
51 derived κ_{CCN} was around 2.4 times larger than the growth factor derived κ_{GF} , which was ascribed to surface tension reduction
52 and solubility limit. Though established thermodynamic models considering surface tension reductions such as compressed
53 film model (Ruehl et al., 2016) and liquid-liquid phase separation model (Ovadnevaite et al., 2017; Liu et al., 2018) explained
54 the discrepancies of CCN activity or CCN number concentration closure, dataset of direct measurement of surface tension for
55 submicron particles are very rare.

56 Dicarboxylic acids are ubiquitous in atmospheric aerosol particle as a main contributor to organic aerosol mass (mass
57 contribution to total particulate carbon ~~could~~ exceeds 10% in remote area) (Römpf et al., 2006; Ho et al., 2010; Hyder et al.,
58 2012). Primary emission (e.g. biomass burning and fossil fuel combustion) and secondary formation (e.g. photooxidation of
59 unsaturated fatty acids) were major sources of dicarboxylic acids (Ho et al., 2010). Furthermore, dicarboxylic acids are also
60 known as important atmospheric surfactants and their surface activities in water solutions showed a positive relation with
61 carbon number (Aumann et al., 2010). Currently, most studies investigated surface tension effect of dicarboxylic acids on CCN
62 activation by measuring surface tension of their solutions and using models based on solution results (Lee and Hildemann,
63 2013, 2014; Ruehl et al., 2016; Zhang et al., 2021; Vepsäläinen et al., 2022). However, the values derived from bulk solutions
64 may not be a reasonable representation for aerosol particles because their high surface-to-volume ratio may affect the

65 distribution of surfactant between surface and bulk (Ruehl et al., 2010; Ruehl and Wilson, 2014). Recently, new methods of
66 surface tension measurement for particles were introduced such as microfluid (Metcalf et al., 2016) and optical tweezers
67 (Bzdek et al., 2020), but their samples were micrometre size droplets. Morris et al. (2015) presented a way to directly measure
68 surface tension of submicron particles under controlled relative humidity (RH) by atomic force microscopy (AFM). Later,
69 AFM was further reported to be an important tool to probe phase state of individual particles (Lee et al., 2017a; Lee et al.,
70 2017b; Lee and Tivanski, 2021). However, most measurements using AFM were performed with RH under 95% (Morris et
71 al., 2015; Lee et al., 2017b; Ray et al., 2019; Lee et al., 2020) but rarely in higher RH conditions. When RH approaches 100%,
72 Kelvin effect becomes comparable to the Raoult effect in controlling hygroscopicity, so measurements around 100% RH can
73 help resolve discrepancies between sub-saturated hygroscopicity and CCN activity (Ruehl and Wilson, 2014).
74 In this study, we firstly measured CCN activities of internal mixtures containing inorganic salt and dicarboxylic acid. Then,
75 we directly obtained their surface tension and phase states by AFM under relatively high RH (over 99.5%). Our results could
76 provide directly dataset of surface tension and phase state of inorganic salts-dicarboxylic acids internal mixed particles, which
77 would help to decrease the uncertainty for climate models.

78 2 Methods

79 2.1 Experiments

80 2.1.1 Chemicals

81 Nine used compounds in the present study were sodium chloride (NaCl), ammonium sulfate (AS), malonic acid (MA),
82 phenylmalonic acid (PhMA), succinic acid (SA), phenylsuccinic acid (PhSA), adipic acid (AA), pimelic acid (PA) and
83 Octanedioic acid (OA). Their relevant properties investigated in this study were summarized in **Table 1**.

84 2.1.2 CCN activity measurements

85 The measurement setup is shown in **Fig. 1**. ~~In brief, particles containing single and mixed chemicals were generated by clean~~
86 ~~and particle-free compressed air with water solutions (~ 1%) by a constant output atomizer (TSI 3079A). The solutions were~~
87 ~~prepared by using ultrapure water (Millipore, resistivity $\leq 18.2\text{M}\Omega$)~~~~In brief, particles containing single and mixed chemicals~~
88 ~~were generated with water solutions (~ 1%) by a constant output atomizer (TSI 3079A).~~ After drying (RH < 15%),
89 monodispersed aerosol particles were obtained by differential mobility analyzer (DMA, TSI 3081) with the sheath to sample
90 flow ratio of 10, and then were split between a condensation particle counter (CPC, TSI 3772) for measuring number
91 concentration of total particles (N_{CN}) and a Cloud Condensation Nuclei Counter (CCNC, DMT-200) for measuring number
92 concentration of CCN (N_{CCN}).

93 In this study, the CCNC was operated in Scanning Flow CCN Analysis (SFCA) mode, which was introduced elsewhere (Moore
94 and Nenes, 2009). In short, the pressure and ΔT of CCNC were kept constant, the flow rate was continuously and linearly

95 varied from 0.2 L min^{-1} to 1 L min^{-1} or vice versa ($1-0.2 \text{ L min}^{-1}$) within 125 s and the interval time for stabilization is 25 s.
96 The supersaturations in CCNC was calibrated under four ΔT (4K, 6K, 10K and 18K). We obtained sigmoidal curves of
97 activation ratio (N_{CCN}/N_{CN}) versus flow rate, then fitted the inflection point of the curves as critical flow rate Q_{50} . Ammonium
98 sulfate was used to determine supersaturation ratio with an activity parameterization Köhler model AP3 as suggested by Rose
99 et al. (2008). The calibration results were showed in **Fig. S1**.

100 2.1.3 Surface tension measurements

101 As shown in **Fig.1**, samples for AFM analysis were collected through deposition by impaction with an eight stage non-
102 viable particle sizing sampler (Models BGI20800 Series, BGI Incorporation) onto hydrophobically silicon wafers. The
103 hydrophobically silicon wafers are with polydimethylsiloxane brush surface, so solute can be collected into the solute
104 aggregate on the surface after water evaporation when RH varies (especially RH decreases) (Ding et al., 2020). The
105 aerodynamic size of collected particles was ranged in $0.4 \mu\text{m}-1 \mu\text{m}$ (50% efficiency). The substrate deposited particles were
106 stored under dry condition ($\text{RH} < 10\%$) and most of the samples were studied at the same day to avoid possible sample aging.
107 Surface tension measurement was performed using an AFM system (Cypher ES, Asylum Research). Cypher ES contains a
108 small cell with air inlet and outlet, it enables to scan samples under different environmental conditions such as RH. RH in cell
109 was achieved and maintained by humidified flow. RH in cell was measured by a RH sensor (SHT 85, $\pm 1.5\%$ uncertainty,
110 Sensirion Inc.). Custom-built high aspect ratio (HAR) platinum AFM probes with constant diameter and nominal spring
111 constant of $\sim 3.0 \text{ N m}^{-1}$ were used for particle imaging and surface tension measurements (**Fig. S2**) (Morris et al., 2015). The
112 platinum nanoneedles could well measure surface tension of pure water and 1, 3-propanediol (**Fig. S3**). The procedures of
113 making nanotips were detailly described in Ding et al. (2022) and a brief description was given here~~The procedures of making~~
114 ~~nanotips were detailly described in a manuscript under review and a brief description was given here.~~ Firstly, dual-beam-
115 focused ion beam (FIB, ZEISS crossbeam 350) microscope was used to etch the top of the tip (Multi75A1-G purchased from
116 BudgetSensors Inc.), making the etched tip flat. Then, FIB was used to deposit a cylindrical metal platinum column ($100 \text{ nm}-$
117 500 nm diameter) on the flat surface of the etched tip.

118 The principles of surface tension measurement using AFM were described elsewhere (Yazdanpanah et al., 2008; Morris et al.,
119 2015; Lee et al., 2017a). Collected samples were firstly imaged in tapping mode to locate individual particles under dry
120 condition ($\text{RH} < 10\%$), then the RH gradually increased to over 99.5% in ~ 40 minutes (**Fig.S4**). Force-distance plots of droplet
121 were obtained by contact mode. A tip velocity of $1-2 \mu\text{m s}^{-1}$ and dwell time of 1-2 seconds were used for all measurements
122 (Kaluarachchi et al., 2021). More than 10 force plots were collected on at least 5 individual droplets in order to decreased the
123 uncertainties (e.g. sensor accuracy). Precise diameter of nanoneedle was calibrated by measuring surface tension of pure water
124 by adding a water droplet (2-3 mm height) onto silicon wafer (Kaluarachchi et al., 2021). New probe was used for different
125 chemicals in order to avoid possible contamination of the AFM probe. However, it should be noted that the potential
126 uncertainty introduced due to the different particle diameter in CCN activity (ranged in 50~260 nm) and AFM experiments

(0.4-1 μ m) is not taken into account, because the size dependence of surface tension is not significant unless the solution droplets are smaller down to 6 nm (Cheng et al., 2015).

2.2 Theory

Based on κ -Köhler theory, hygroscopicity parameter κ_{CCN} for individual pure component and mixed aerosol can be calculated by:

$$\kappa_{\text{CCN}} = \frac{4A^3}{27D_d^3 \ln^2(1+s_c)}, A = \frac{4M_w \sigma_w}{RT \rho_w} \quad (1)$$

where σ_w , M_w and ρ_w are surface tension, molecular weight and density of water, respectively. R is universal gas constant and T is temperature (298.15K). s_c is critical supersaturation ratio. D_d is dry diameter. In addition, hygroscopicity κ of multicomponent chemical system can also be calculated assuming a Zdanovskii, Stokes, and Robinson (ZSR) simple mixing rule. κ based on the chemical composition (κ_{Chem}) of mixed aerosol was calculated by:

$$\kappa_{\text{Chem}} = \text{OVF} \cdot \kappa_{\text{org,CCN}} + (1 - \text{OVF}) \cdot \kappa_{\text{inorg,CCN}} \quad (2)$$

where $\kappa_{\text{org,CCN}}$ and $\kappa_{\text{inorg,CCN}}$ are obtained hygroscopicity κ values (here obtained κ_{CCN} values were used) values of single organic acids and inorganic salts. OVF indicates the organic volume fraction of mixed particles

As described by Morris et al. (2015), the basis of surface tension measurement for a liquid droplet by AFM was calculated by:

$$\sigma = \frac{F_r}{2\pi r} \quad (3)$$

where F_r is the retention force to break the meniscus by the tip of AFM probe, r is the radius of the AFM probe tip, and σ is surface tension of the droplet. The retention force is the force difference before and after the probe was just retracted from the droplet.

3 Results and discussion

3.1 κ_{CCN} of single component

κ_{CCN} values for single component aerosols were summarized in **Table 2**. κ_{CCN} of NaCl, AS, MA, SA and AA were 1.325 ± 0.038 , 0.562 ± 0.059 , 0.240 ± 0.036 , 0.204 ± 0.023 and 0.008 ± 0.001 , respectively, being overall consistent with previous results (Petters and Kreidenweis, 2007; Kuwata et al., 2013). κ_{CCN} of NaCl and MA were slightly higher while AS was slightly lower than those reported in Petters and Kreidenweis (2007). This may be ascribed to the solute purity (Hings et al., 2008). Based on the same reason, κ_{CCN} of PA (0.112 ± 0.010) and OA (0.003 ± 0.0002) were 20% lower and twice higher than those reported by Kuwata et al. (2013), respectively. PA and OA were 0.112 ± 0.010 and 0.003 ± 0.0002 , which were 20% lower and

twice higher than those reported by Kuwata et al. (2013). Possible factor may be the purity of solutes, because additional hydrophobic (or hygroscopic) matters in commercial reagents may possibly decrease (increase) organic hygroscopicity (Hings et al., 2008). κ_{CCN} values of PhMA and PhSA were 0.183 ± 0.032 and 0.145 ± 0.017 , respectively, which ~~to our knowledge are was~~ firstly reported ~~to our knowledge in this study~~.

Solubility and molar volume of dicarboxylic acids were essential factors influencing their hygroscopicity (Kumar et al., 2003; Han et al., 2022). ~~Therefore, solubility criteria of 100 g/L was used in our study to distinguish the effect of solubility of highly soluble (with water solubility over 100 g L⁻¹) and slightly soluble organics (with water solubility below 100 g L⁻¹) on their hygroscopicity, according to Kuwata et al. (2013) and Luo et al. (2020). In this study, we considered two regimes: highly soluble organic components (with water solubility over 100 g L⁻¹) and slightly soluble organic components (with water solubility between 10-100 g L⁻¹), which was consistent with previous study (Kuwata et al., 2013).~~ As showed in **Fig. 2a**, the κ_{CCN} values for highly soluble components decreased linearly with increased molecular volumes. This trend was similar to κ_{CCN} values for sugar as well as dicarboxylic acids reported by Chan et al. (2008). In **Fig. 2b**, κ_{CCN} values of sparsely soluble components (AA, PA, SA and OA) showed an increased trend with solubility, as organic matter with the higher water solubility would dissolve more and have a higher molar concentration, resulting in reduction in water activity and higher hygroscopicity (Luo et al., 2020; Han et al., 2022).

Organic functional group could also affect hygroscopicity (Suda et al., 2014; Petters et al., 2017). κ_{CCN} of PA (0.112) was higher than those of AA (0.008) and OA (0.003), which is contrary to results in Suda et al. (2014) and Petters et al. (2017) that hygroscopicity decreased with increased number of methylene. This phenomenon was attributed to the odd-even effect of dicarboxylic acids, that is, diacids with odd numbers of carbon atoms being more soluble than those with adjacent even numbers (Zhang et al., 2013). Furthermore, κ_{CCN} values of PhMA and PhSA were both lower than that of MA and SA, respectively, indicating that the addition of phenyl showed negative effects on hygroscopicity. The addition of phenyl substitution increased the molar volumes of MA and SA and may contribute to the drops of hygroscopicity (Petters et al., 2009).

3.2 κ_{CCN} of inorganic salt-dicarboxylic acid mixed components

Figure 3 presents the κ_{CCN} values of inorganic salt/dicarboxylic acid mixed particles with varied organic volume fractions (OVF). Overall, κ_{CCN} of each inorganic salt/dicarboxylic acid system showed a decreased trend with increased OVF. For example, κ_{CCN} of AS/MA particles with OVF of 57%, 73% and 88% were 0.399, 0.373 and 0.336, respectively. Larger fractions of dicarboxylic acids (with low hygroscopicity compares to inorganic salts) caused more decrease in hygroscopicity of inorganic/dicarboxylic acid system. As for inorganic salt/dicarboxylic acid systems with same OVF, κ_{CCN} values of systems of AS/MA, AS/SA, AS/PhMA, AS/PhSA and AS/PA with 57% OVF were 0.399, 0.382, 0.364, 0.340 and 0.334, following the order of κ_{CCN} values of single dicarboxylic acid (**Fig. 3a**). However, κ_{CCN} values of NaCl/AA and NaCl/OA mixed particles with OVF of 60% were 0.734 and 0.685, even higher than that of NaCl/MA (0.639), demonstrating an opposite trend with

186 respect to those of single components. This discrepancy could be ascribed to surface tension reduction because AA and OA
187 showed different physical properties (e.g. deliquescence point, surface activity and solubility) when comparing with the other
188 organics, thus may result in distinct microphysics processes during interactions with inorganic salts and water content. AA and
189 OA own lowest solubilities and high deliquescence RH (**Table1**) among experimental dicarboxylic acids, which potentially
190 lead to their weak CCN activities (Hings et al., 2008). However, inorganic salts were found to facilitate the deliquescence of
191 dicarboxylic acid (Bilde and Svenningsson, 2004; Sjogren et al., 2007; Minambres et al., 2013). AS/AA mixed particles
192 deliquescence under 78%-83% RH with mass fractions of AA between 50%-80% (Sjogren et al., 2007). Small amount of NaCl
193 (2% mass fraction) could notably decrease s_c of AA with 80 nm dry diameter from over 2% to ~0.6% (Bilde and Svenningsson,
194 2004). Thus, addition of inorganic salts facilitates deliquescence of OA and AA under lower RH, further promotes their phase
195 state transition from solid to liquid (or semisolid), and their surface tension would be reduced. Based on surface tension results
196 of water solutions, Aumann et al. (2010) reported that surface activities of dicarboxylic acids were increased with their carbon
197 number. Therefore, surface tensions of inorganic salts/AA and inorganic salts/OA may decrease more than the rest acids
198 containing particles, resulting in their relatively higher κ_{CCN} , which may further promote phase state transition from solid to
199 liquid (or semisolid) and cause surface tension reductions as OA and AA show stronger surface activities than most of the rest
200 dicarboxylic acids because of longer carbon chain (Aumann et al., 2010). This indication was further confirmed by AFM
201 surface tension measurement, as discussed in Section 3.4.

202 3.3 Closure study between κ_{CCN} and κ_{Chem}

203 κ_{CCN} and κ_{Chem} values for inorganic salt/dicarboxylic acid mixed particles were showed in **Fig. 4**. κ_{CCN} values of inorganic salt
204 and most dicarboxylic acids (MA, PhMA, SA, PhSA and PA) mixed particles could be predicted by ZSR mixing rule with
205 relative difference below 30% (**Fig. 4a**). Similar results have been found in previous lab and filed studies (Ruehl et al., 2012;
206 Kuwata et al., 2013; Wu et al., 2013; Dawson et al., 2016; Nguyen et al., 2017; Ovadnevaite et al., 2017), indicating that semi-
207 experimental ZSR mixing rule could be a useful method to predicted mixed particles hygroscopicity and CCN activation. For
208 instance, Dawson et al. (2016) reported consistence between κ_{CCN} and κ_{Chem} for NaCl/xanthan gum and CaCO₃/xanthan gum
209 mixed particles within 10% uncertainty. Wu et al. (2013) also obtained same closure results in a field study at central Germany,
210 for particles containing 60%-80% organic mass fraction and 30%-50% inorganic salts. Meanwhile, CCN studies also found
211 that using κ_{Chem} could well predict measured CCN number concentration (Juranyi et al., 2010; Rose et al., 2010; Almeida et
212 al., 2014; Kawana et al., 2016; Cai et al., 2020; Zhang et al., 2020). However, for inorganic/AA and inorganic/OA mixed
213 particles (**Fig. 4b**), their κ_{CCN} values were 0.3-3.0 times higher than κ_{Chem} . Surface tension reduction was one of the potential
214 causes, as discussed in section 3.2 that OA and AA with strong surface activity and low solubilities may result in stronger
215 surface tension reduction than most of the rest dicarboxylic acids. In addition, the underprediction showed a gradual increased
216 trend with increased OVF since increased OVF lead to higher concentration of organics, thus leading to more surface tension
217 reduction. Surface tension reduction in water solution caused by atmospheric surfactants were observed frequently in previous

218 studies (Facchini et al., 1999; Gerard et al., 2016). Results have showed that neglect of surface tension reduction may lead to
219 higher κ_{CCN} values than κ_{Chem} or growth factor derived κ_{GF} (Irwin et al., 2010; Wu et al., 2013; Zhao et al., 2016; Hu et al.,
220 2020; Peng et al., 2021), as well as underpredictions of CCN number concentration (Good et al., 2010; Asa-Awuku et al., 2011;
221 Ovadnevaite et al., 2017; Cai et al., 2020). Hu et al. (2020) reported that κ_{Chem} underpredicted κ_{CCN} by 13% and 18% at
222 supersaturation ratios of 0.1% and 0.3%, which may be attributed to the depression of droplet surface tension by potential
223 surface-active organics. Likewise, Ovadnevaite et al. (2017) only predicted one tenth of measured CCN number concentration
224 in a nascent ultrafine mode event because of the surface tension reduction, and the notable underestimation was improved by
225 applying lower water surface tension ($\sim 68\%$ of water surface tension) in κ -Köhler theory.

226 Apart from surface tension reduction, aerosol phase states could also bring uncertainty to critical supersaturation and
227 hygroscopicity predictions (Henning et al., 2005; Hodas et al., 2015; Peng et al., 2016; Zhao et al., 2016). Being different from
228 tradition Köhler curve with only one maximum, modified Köhler curve for inorganic salt and slightly soluble dicarboxylic
229 acid (e.g. AA) mixed particles accounting for limited solubility obtained two maxima of critical supersaturation ratios and the
230 higher value among the two maxima determined CCN activation (Bilde and Svenningsson, 2004). The maximum at the larger
231 wet diameter is identical with that obtained by assuming that the organic acids are infinitely soluble in water (i.e. classical
232 Köhler theory). And the other maximum with smaller wet diameter represents the point that all slightly soluble material is
233 fully dissolved and the maximum can also be viewed as an activation barrier which is due to the presence of a undissolved
234 solid part of organic acid (Henning et al., 2005). Pajunoja et al. (2015) reported that biogenic secondary organic aerosol (SOA)
235 particles formed from isoprene showed an increased trend of hygroscopicity parameter from 0.05 to nearly 0.15 when RH
236 increased from 40% to supersaturation. They indirectly found the biogenic SOA to be semisolid phase thus the increased trend
237 of hygroscopicity κ was explained by the gradual phase transition from solid to semisolid (or liquid) with raised RH because
238 water content may gradually wet and dissolve the organic surface and form water film (Pajunoja et al., 2015). The phase
239 transition (or water film formation) of pure OA and AA would be difficult (i.e. high RH is required) because of their high
240 deliquescence point and low solubilities, but could be easier (i.e. required high RH is decreased) by addition of inorganic salts.
241 Overall, phase state and surface tension of atmospheric aerosol were two essential factors influencing their hygroscopicity and
242 CCN activation. Though there are several indirect ways detecting aerosol phase state (Pajunoja et al., 2015; Shiraiwa et al.,
243 2017), current studies about direct measurements are still very limited.

244 **3.4 Phase state and surface tension of inorganic salt/dicarboxylic acid mixed particles**

245 **3.4.1 Phase state**

246 We obtained phase states of inorganic salt/dicarboxylic acid under high RH ~~environment~~(over 99.5%) by analyzing shapes of
247 force plot based on AFM system (Lee et al., 2017a; Lee and Tivanski, 2021). **Figure 5a** shows ~~sed~~ force plot of NaCl/MA mixed
248 particles with 75% OVF. AFM probe needle tip approached the droplet vertically before contacting with droplet, needle tip
249 was not disturbed by extra force (red line). Then, needle tip came in contact with the droplet, resulting in an abrupt negative

250 force (i.e. needle was attracting by drop). After that, needle moved through the droplet with negative force until contacting
251 with the substrate. When tip contacted substrate, the negative force would quickly be positive (repulsive force), exceeding a
252 predefined maximum amount of force. Then the tip retracted back away from the droplet, as indicates by blue line. Because
253 of the surface tension of droplet surface, needle tip would experience attractive force and abruptly turned to zero when tip
254 separated from droplet surface. Our observation in **Fig. 5a** showed a similar shape with results reported by Morris et al. (2015),
255 indicating the particles were liquid. Most of the studied inorganic salt/dicarboxylic acid (MA, PhMA, SA, PhSA and PA) were
256 liquid under RH over 99.5%.

257 However, for AS/SA (72% and 88% OVF), NaCl/AA (89% OVF), AS/AA (57%, 72% and 88% OVF) and AS/OA (88%
258 OVF), the shape force plots were totally different. During the tip contacting with particle, force plots showing a jagging profile,
259 as shown in **Fig. 5b**. This shape is nearly the same as the curves for NaBr particles under 52% RH reported by Lee et al.
260 (2017a). They explained the phase of NaBr was semi-solid and jagging profile in tip approaching was caused by its viscosity.
261 Therefore, AS/SA (72% and 88% OVF), NaCl/AA (89% OVF), AS/AA (57%, 72% and 88% OVF) and AS/OA (88% OVF)
262 mixed particles were indicated to be semisolid. Semisolid phase states were more likely to occur when containing higher OVF
263 of dicarboxylic acids with lower solubilities and higher deliquescence point (SA, AA and OA) and inorganic salts with
264 comparative lower hygroscopicity (AS), as in this circumstance water content may be insufficient and could not easily dissolve
265 organics. Therefore, semisolid phase of inorganic salt/AA and inorganic salt/OA mixed particles provides evident for phase
266 state effect on aerosol hygroscopicity, which may be attributable to higher κ_{CCN} than κ_{Chem} as discussed in section 3.3 (**Fig**
267 **4b**). Though AS/SA mixed particles (72% and 88% OVF) were semisolid because of high deliquescence point (98%) of SA,
268 their good closure between κ_{CCN} and κ_{Chem} may be ascribed to higher solubility of SA, which may intensify the water absorption
269 after deliquescence thus phase transition from semisolid to diluted liquid when activating to CCN.

270 **3.4.2 Surface tension**

271 Lee et al. (2017a) pointed out that surface tension calculation could not be achieved for semisolid particles, because the
272 measured retention force was not solely attributed to surface tension, but have additional contributions that include viscosity.
273 Therefore, only surface tensions of inorganic salt/dicarboxylic acid mixed particles that were liquid were further obtained by
274 **Eq.3**. Surface tension results were summarized in **Fig. 6**. Overall, surface tensions of all inorganic salt/dicarboxylic acid mixed
275 particles showed a decrease trend with increased OVF as higher OVF may result in higher organic solute concentrations thus
276 caused more surface tension reduction. Surface tensions of inorganic salts mixed with MA, PhMA, SA, PhSA and PA lowered
277 by within 12% than that of pure water (72 mN m^{-1}), indicating that droplets got strongly diluted at RH over 99.5%, and ought
278 to be more diluted when activation occurs. This may contribute to κ closure within 30% deviation in **Fig. 4a** because diluted
279 solution and water surface tension were assumed in κ -Köhler theory. However, surface tensions of inorganic salts/AA and
280 inorganic salts/OA mixed particles showed notable reductions (20%-42%), which may contribute to their higher κ_{CCN} values
281 than κ_{Chem} (**Fig. 4b**). Besides, notable surface tension reductions of particles containing OA or AA indicated that organic

282 solubility plays an important role in surface tension reduction as AA and OA have the lowest solubilities among studied
283 dicarboxylic acids. OA and AA own higher carbon numbers than most of the rest studied organics. Since Aumann et al. (2010)
284 found that the surface activity of dicarboxylic acids increases with carbon number from 2 to 9 based on surface tension
285 measurement of their water solutions, indicating that dicarboxylic acids (e.g. OA and AA) with higher carbon number own
286 stronger surface activity. Therefore, strong surface activity of dicarboxylic acid is another factor attributing to surface tension
287 reduction of inorganic salts/dicarboxylic acids. Besides, OA and AA own higher deliquescence point and longer carbon chains
288 than most of the rest studied organics and thus deliquescence RH and strong surface activity are also essential factors attributing
289 to surface tension reduction for inorganic salt/dicarboxylic acid mixed particles. Furthermore, for dicarboxylic acids, lower
290 organic solubilities may be more important factor causing surface tension reduction than deliquescence RH and surface activity.
291 This was because PA with higher solubility, but similar deliquescence RH and surface activity like AA and OA did not show
292 much depression of surface tension when mixed with inorganic salts.

293 4 Conclusions

294 The role of surfactants such as dicarboxylic acids in CCN activity were often ignored in aerosol hygroscopicity studies and
295 currently used climate models. In this study, we analyzed CCN activities of inorganic salt/dicarboxylic acid internal mixed
296 particles with varied OVF and directly measured their phase state and surface tension by AFM under relative high RH.

297 κ_{CCN} values of single dicarboxylic acid were located in the range of 0.003-0.240. A linearly positive correlation between κ_{CCN}
298 and solubility were-was obtained for slightly dissolved species, while a negative correlation was found between κ_{CCN} and
299 molecular volume for highly soluble species. κ_{CCN} of PhMA and PhSA were lower than those of MA and SA, respectively,
300 revealing that addition of phenyl radical could weaken hygroscopicity of dicarboxylic acid.

301 For most inorganic salt/dicarboxylic acid (MA, PhMA, SA, PhSA and PA), κ_{CCN} of mixed particles with same OVF showed
302 an overall decrease trend and followed the order of κ_{CCN} values of single dicarboxylic acid. Good closure within 30% relative
303 bias between κ_{CCN} and κ_{Chem} were obtained. On the contrast, our results demonstrated that the semisolid phase state and surface
304 tension reduction (20%-42%) are the potential factors to explain the enhanced CCN activity of inorganic salts/OA and
305 inorganic salts/AA mixed particles. Slightly dissolved dicarboxylic acids with lower solubilities, higher deliquescence point
306 and strong surface activity are more likely to cause notable surface tension depression for inorganic salt/dicarboxylic acid mix
307 particles. Therefore, we proposed that surface tension reduction and phase state should be carefully considered in future models
308 and observations, especially for slightly soluble organics with lower solubilities, high deliquescence RH and strong surface
309 activity.

310
311 **Data availability.** The data used in this paper can be obtained from the corresponding author upon request.

312 **Author contributions.** CX did the experiments, analyzed data, plotted the figures and wrote the original draft. BYK contributed
313 data analyzing and discussion, reviewed the manuscript and contributed to fund acquisition. XYC, XLD, ~~and~~ XYP and SKY
314 contributed to the instrumentation and discussion. ZNX contributed to the discussion and fund acquisition. HH contributed to
315 the instrumentation, discussion and fund acquisition. ZBW administrated the project, conceptualized the study, reviewed the
316 manuscript and contributed to fund acquisition.

317 **Acknowledgment.** The research was supported by National Natural Science Foundation of China (91844301, 42005087,
318 61974128 and 42005086) and the Fundamental Research Funds for the Central Universities (2018QNA6008). We thank Dr.
319 Lin Liu from Instrumentation and Service Center for Physical Sciences at Westlake University for the supporting in AFM
320 experiments. We likewise appreciate Shikuan Yang, Qianqian Ding and Xueyan Chen for making and kindly sharing
321 hydrophobically silicene wafers. We likewise thank Dr. ~~Ren~~ Zhu and Dr. Zhiwen Liu at Oxford Instruments, Dr. Lin Liu,
322 Renwei Mao at Zhejiang university and Dr. Yuzhong Zhang at Westlake University for the discussions about AFM experiment.

323 **Competing interests.** The authors declare no competing financial interest.

324 **References**

- 325 Almeida, G. P., Brito, J., Morales, C. A., Andrade, M. F., and Artaxo, P.: Measured and modelled cloud condensation
326 nuclei (CCN) concentration in Sao Paulo, Brazil: the importance of aerosol size-resolved chemical composition on
327 CCN concentration prediction, *Atmos. Chem. Phys.*, 14, 7559-7572, <https://doi.org/10.5194/acp-14-7559-2014>,
328 2014.
- 329 Asa-Awuku, A., Moore, R. H., Nenes, A., Bahreini, R., Holloway, J. S., Brock, C. A., Middlebrook, A. M., Ryerson, T.
330 B., Jimenez, J. L., DeCarlo, P. F., Hecobian, A., Weber, R. J., Stickel, R., Tanner, D. J., and Huey, L. G.: Airborne
331 cloud condensation nuclei measurements during the 2006 Texas Air Quality Study, *J. Geophys. Res.: Atmos.*, 116,
332 D11201, <https://doi.org/10.1029/2010jd014874>, 2011.
- 333 Aumann, E., Hildemann, L. M., and Tabazadeh, A.: Measuring and modeling the composition and temperature-
334 dependence of surface tension for organic solutions, *Atmos. Environ.*, 44, 329-337,
335 <https://doi.org/10.1016/j.atmosenv.2009.10.033>, 2010.
- 336 Bhattu, D. and Tripathi, S. N.: CCN closure study: Effects of aerosol chemical composition and mixing state, *J Geophys*
337 *Res-Atmos*, 120, 766-783, <https://doi.org/10.1002/2014jd021978>, 2015.
- 338 Bilde, M. and Svenningsson, B.: CCN activation of slightly soluble organics: the importance of small amounts of
339 inorganic salt and particle phase, *Tellus B: Chem. Phys. Meteorol.*, 56, 128-134,
340 <https://doi.org/10.3402/tellusb.v56i2.16406>, 2004.
- 341 Bzdek, B. R., Reid, J. P., Malila, J., and Prisle, N. L.: The surface tension of surfactant-containing, finite volume droplets,
342 *Proc. Natl. Acad. Sci. U.S.A.*, 117, 8335-8343, <https://doi.org/10.1073/pnas.1915660117>, 2020.
- 343 Cai, M., Liang, B., Sun, Q., Zhou, S., Chen, X., Yuan, B., Shao, M., Tan, H., and Zhao, J.: Effects of continental
344 emissions on cloud condensation nuclei (CCN) activity in the northern South China Sea during summertime 2018,
345 *Atmos. Chem. Phys.*, 20, 9153-9167, <https://doi.org/10.5194/acp-20-9153-2020>, 2020.
- 346 Chan, M. N., Kreidenweis, S. M., and Chan, C. K.: Measurements of the hygroscopic and deliquescence properties of
347 organic compounds of different solubilities in water and their relationship with cloud condensation nuclei activities,
348 *Environ. Sci. Technol.*, 42, 3602-3608, <https://doi.org/10.1021/es7023252>, 2008.
- 349 Cheng, Y. F., Su, H., Koop, T., Mikhailov, E., and Poschl, U.: Size dependence of phase transitions in aerosol
350 nanoparticles, *Nat. Commun.*, 6, <https://doi.org/10.1038/ncomms6923>, 2015.

351 Dawson, K. W., Petters, M. D., Meskhidze, N., Petters, S. S., and Kreidenweis, S. M.: Hygroscopic growth and cloud
352 droplet activation of xanthan gum as a proxy for marine hydrogels, *J. Geophys. Res.: Atmos.*, 121, 11803–11818,
353 <https://doi.org/10.1002/2016jd025143>, 2016.

354 Ding, Q., Wang, J., Chen, X., Liu, H., Li, Q., Wang, Y., and Yang, S.: Quantitative and sensitive SERS platform with
355 analyte enrichment and filtration function, *Nano Lett.*, 20, 7304–7312, <https://doi.org/10.1021/acs.nanolett.0c02683>,
356 2020.

357 Ding, X., Kuang, B., Xiong, C., Mao, R., Xu, Y., Wang, Z., and Hu, H.: A Super High Aspect Ratio Atomic Force
358 Microscopy Probe for Accurate Topography and Surface Tension Measurement, *Sens. Actuators, A*, 113891,
359 <https://doi.org/10.1016/j.sna.2022.113891>, 2022.

360 Dusek, U., Frank, G. P., Hildebrandt, L., Curtius, J., Schneider, J., Walter, S., Chand, D., Drewnick, F., Hings, S., Jung,
361 D., Borrmann, S., and Andreae, M. O.: Size matters more than chemistry for cloud-nucleating ability of aerosol
362 particles, *Science*, 312, 1375–1378, <https://doi.org/10.1126/science.1125261>, 2006.

363 Facchini, M. C., Mircea, M., Fuzzi, S., and Charlson, R. J.: Cloud albedo enhancement by surface-active organic solutes
364 in growing droplets, *Nature*, 401, 257–259, <https://doi.org/10.1038/45758>, 1999.

365 Gerard, V., Noziere, B., Baduel, C., Fine, L., Frossard, A. A., and Cohen, R. C.: Anionic, Cationic, and Nonionic
366 Surfactants in Atmospheric Aerosols from the Baltic Coast at Asko, Sweden: Implications for Cloud Droplet
367 Activation, *Environ Sci Technol*, 50, 2974–2982, <https://doi.org/10.1021/acs.est.5b05809>, 2016.

368 Good, N., Topping, D. O., Allan, J. D., Flynn, M., Fuentes, E., Irwin, M., Williams, P. I., Coe, H., and McFiggans, G.:
369 Consistency between parameterisations of aerosol hygroscopicity and CCN activity during the RHaMBLe
370 discovery cruise, *Atmos. Chem. Phys.*, 10, 3189–3203, <https://doi.org/10.5194/acp-10-3189-2010>, 2010.

371 Gunthe, S. S., King, S. M., Rose, D., Chen, Q., Roldin, P., Farmer, D. K., Jimenez, J. L., Artaxo, P., Andreae, M. O.,
372 Martin, S. T., and Pöschl, U.: Cloud condensation nuclei in pristine tropical rainforest air of Amazonia: size-
373 resolved measurements and modeling of atmospheric aerosol composition and CCN activity, *Atmos. Chem. Phys.*,
374 9, 7551–7575, <https://doi.org/10.5194/acp-9-7551-2009>, 2009.

375 Han, S., Hong, J., Luo, Q., Xu, H., Tan, H., Wang, Q., Tao, J., Zhou, Y., Peng, L., He, Y., Shi, J., Ma, N., Cheng, Y.,
376 and Su, H.: Hygroscopicity of organic compounds as a function of organic functionality, water solubility, molecular
377 weight, and oxidation level, *Atmos. Chem. Phys.*, 22, 3985–4004, <https://doi.org/10.5194/acp-22-3985-2022>, 2022.

378 Henning, S., Rosenorn, T., D'Anna, B., Gola, A. A., Svenningsson, B., and Bilde, M.: Cloud droplet activation and
379 surface tension of mixtures of slightly soluble organics and inorganic salt, *Atmos. Chem. Phys.*, 5, 575–582,
380 <https://doi.org/10.5194/acp-5-575-2005>, 2005.

381 Hings, S. S., Wrobel, W. C., Cross, E. S., Worsnop, D. R., Davidovits, P., and Onasch, T. B.: CCN activation experiments
382 with adipic acid: effect of particle phase and adipic acid coatings on soluble and insoluble particles, *Atmos. Chem.*
383 *Phys.*, 8, 3735–3748, <https://doi.org/10.5194/acp-8-3735-2008>, 2008.

384 Ho, K. F., Lee, S. C., Ho, S. S. H., Kawamura, K., Tachibana, E., Cheng, Y., and Zhu, T.: Dicarboxylic acids,
385 ketocarboxylic acids, α -dicarbonyls, fatty acids, and benzoic acid in urban aerosols collected during the 2006
386 Campaign of Air Quality Research in Beijing (CAREBeijing-2006), *J. Geophys. Res.: Atmos.*, 115, D19312,
387 <https://doi.org/10.1029/2009jd013304>, 2010.

388 Hodas, N., Zuend, A., Mui, W., Flagan, R. C., and Seinfeld, J. H.: Influence of particle-phase state on the hygroscopic
389 behavior of mixed organic–inorganic aerosols, *Atmos. Chem. Phys.*, 15, 5027–5045, <https://doi.org/10.5194/acp-15-5027-2015>, 2015.

391 Hu, D., Liu, D., Zhao, D., Yu, C., Liu, Q., Tian, P., Bi, K., Ding, S., Hu, K., Wang, F., Wu, Y., Wu, Y., Kong, S., Zhou,
392 W., He, H., Huang, M., and Ding, D.: Closure investigation on cloud condensation nuclei ability of processed
393 anthropogenic aerosols, *J. Geophys. Res.: Atmos.*, 125, e2020JD032680, <https://doi.org/10.1029/2020jd032680>,
394 2020.

395 Hyder, M., Genberg, J., Sandahl, M., Swietlicki, E., and Jönsson, J. Å.: Yearly trend of dicarboxylic acids in organic
396 aerosols from south of Sweden and source attribution, *Atmos. Environ.*, 57, 197–204,
397 <https://doi.org/10.1016/j.atmosenv.2012.04.027>, 2012.

398 Irwin, M., Good, N., Crosier, J., Choularton, T. W., and McFiggans, G.: Reconciliation of measurements of hygroscopic
399 growth and critical supersaturation of aerosol particles in central Germany, *Atmos. Chem. Phys.*, 10, 11737-11752,
400 <https://doi.org/10.5194/acp-10-11737-2010>, 2010.

401 Juranyi, Z., Gysel, M., Weingartner, E., DeCarlo, P. F., Kammermann, L., and Baltensperger, U.: Measured and
402 modelled cloud condensation nuclei number concentration at the high alpine site Jungfraujoch, *Atmos. Chem. Phys.*,
403 10, 7891-7906, <https://doi.org/10.5194/acp-10-7891-2010>, 2010.

404 Kaluarachchi, C. P., Lee, H. D., Lan, Y., Lansakara, T. I., and Tivanski, A. V.: Surface tension measurements of aqueous
405 liquid-air interfaces probed with microscopic indentation, *Langmuir*, 37, 2457-2465,
406 <https://doi.org/10.1021/acs.langmuir.0c03507>, 2021.

407 Kawana, K., Nakayama, T., and Mochida, M.: Hygroscopicity and CCN activity of atmospheric aerosol particles and
408 their relation to organics: Characteristics of urban aerosols in Nagoya, Japan, *J. Geophys. Res.: Atmos.*, 121, 4100-
409 4121, <https://doi.org/10.1002/2015jd023213>, 2016.

410 Köhler, H.: The nucleus in and the growth of hygroscopic droplets, *Trans. Faraday Soc.*, 32, 1152-1161,
411 <https://doi.org/10.1039/tf9363201152>, 1936.

412 Kumar, P. P., Broekhuizen, K., and Abbatt, J. P. D.: Organic acids as cloud condensation nuclei: Laboratory studies of
413 highly soluble and insoluble species, *Atmos. Chem. Phys.*, 3, 509-520, <https://doi.org/10.5194/acp-3-509-2003>,
414 2003.

415 Kuwata, M., Shao, W., Lebouteiller, R., and Martin, S. T.: Classifying organic materials by oxygen-to-carbon elemental
416 ratio to predict the activation regime of Cloud Condensation Nuclei (CCN), *Atmos. Chem. Phys.*, 13, 5309-5324,
417 <https://doi.org/10.5194/acp-13-5309-2013>, 2013.

418 Lee, H. D., Estillore, A. D., Morris, H. S., Ray, K. K., Alejandro, A., Grassian, V. H., and Tivanski, A. V.: Direct surface
419 tension measurements of individual sub-micrometer particles using atomic force microscopy, *J. Phys. Chem. A*,
420 121, 8296-8305, <https://doi.org/10.1021/acs.jpca.7b04041>, 2017a.

421 Lee, H. D., Ray, K. K., and Tivanski, A. V.: Solid, semisolid, and liquid phase states of individual submicrometer
422 particles directly probed using atomic force microscopy, *Anal. Chem.*, 89, 12720-12726,
423 <https://doi.org/10.1021/acs.analchem.7b02755>, 2017b.

424 Lee, H. D., Morris, H. S., Laskina, O., Sultana, C. M., Lee, C., Jayarathne, T., Cox, J. L., Wang, X., Hasenecz, E. S.,
425 DeMott, P. J., Bertram, T. H., Cappa, C. D., Stone, E. A., Prather, K. A., Grassian, V. H., and Tivanski, A. V.:
426 Organic enrichment, physical phase state, and surface tension depression of nascent core-shell sea spray aerosols
427 during two phytoplankton blooms, *ACS Earth Space Chem.*, 4, 650-660,
428 <https://doi.org/10.1021/acsearthspacechem.0c00032>, 2020.

429 Lee, H. D. and Tivanski, A. V.: Atomic force microscopy: An emerging tool in measuring the phase state and surface
430 tension of individual aerosol particles, *Annu. Rev. Phys. Chem.*, 72, 235-252, <https://doi.org/10.1146/annurev-physchem-090419-110133>, 2021.

432 Lee, J. Y. and Hildemann, L. M.: Surface tension of solutions containing dicarboxylic acids with ammonium sulfate, d-
433 glucose, or humic acid, *J. Aerosol Sci.*, 64, 94-102, <https://doi.org/10.1016/j.jaerosci.2013.06.004>, 2013.

434 Lee, J. Y. and Hildemann, L. M.: Surface tensions of solutions containing dicarboxylic acid mixtures, *Atmos. Environ.*,
435 89, 260-267, <https://doi.org/10.1016/j.atmosenv.2014.02.049>, 2014.

436 Liu, P. F., Song, M. J., Zhao, T. N., Gunthe, S. S., Ham, S. H., He, Y. P., Qin, Y. M., Gong, Z. H., Amorim, J. C.,
437 Bertram, A. K., and Martin, S. T.: Resolving the mechanisms of hygroscopic growth and cloud condensation nuclei
438 activity for organic particulate matter, *Nat. Commun.*, 9, 4076, <https://doi.org/10.1038/s41467-018-06622-2>, 2018.

439 Lowe, S. J., Partridge, D. G., Davies, J. F., Wilson, K. R., Topping, D., and Riipinen, I.: Key drivers of cloud response
440 to surface-active organics, *Nat. Commun.*, 10, 5214, <https://doi.org/10.1038/s41467-019-12982-0>, 2019.

441 Luo, Q. W., Hong, J., Xu, H. B., Han, S., Tan, H. B., Wang, Q. Q., Tao, J. C., Ma, N., Cheng, Y. F., and Su, H.:
442 Hygroscopicity of amino acids and their effect on the water uptake of ammonium sulfate in the mixed aerosol
443 particles, *Sci. Total Environ.*, 734, 139318, <https://doi.org/10.1016/j.scitotenv.2020.139318>, 2020.

444 Metcalf, A. R., Boyer, H. C., and Dutcher, C. S.: Interfacial tensions of aged organic aerosol particle mimics using a
445 biphasic microfluidic platform, *Environ. Sci. Technol.*, 50, 1251-1259, <https://doi.org/10.1021/acs.est.5b04880>,
446 2016.

447 Minambres, L., Mendez, E., Sanchez, M. N., Castano, F., and Basterretxea, F. J.: Water uptake of internally mixed
448 ammonium sulfate and dicarboxylic acid particles probed by infrared spectroscopy, *Atmos. Environ.*, 70, 108-116,
449 <https://doi.org/10.1016/j.atmosenv.2013.01.007>, 2013.

450 Moore, R. H. and Nenes, A.: Scanning Flow CCN Analysis—A Method for Fast Measurements of CCN Spectra, *Aerosol*
451 *Sci. Technol.*, 43, 1192-1207, <https://doi.org/10.1080/02786820903289780>, 2009.

452 Morris, H. S., Grassian, V. H., and Tivanski, A. V.: Humidity-dependent surface tension measurements of individual
453 inorganic and organic submicrometre liquid particles, *Chem. Sci.*, 6, 3242-3247,
454 <https://doi.org/10.1039/c4sc03716b>, 2015.

455 Nguyen, Q. T., Kjær, K. H., Kling, K. I., Boesen, T., and Bilde, M.: Impact of fatty acid coating on the CCN activity of
456 sea salt particles, *Tellus B: Chem. Phys. Meteorol.*, 69, <https://doi.org/10.1080/16000889.2017.1304064>, 2017.

457 Noziere, B.: Don't forget the surface, *Science*, 351, 1396-1397, <https://doi.org/10.1126/science.aaf3253>, 2016.

458 Ovadnevaite, J., Zuend, A., Laaksonen, A., Sanchez, K. J., Roberts, G., Ceburnis, D., Decesari, S., Rinaldi, M., Hodas,
459 N., Facchini, M. C., Seinfeld, J. H., and C, O. D.: Surface tension prevails over solute effect in organic-influenced
460 cloud droplet activation, *Nature*, 546, 637-641, <https://doi.org/10.1038/nature22806>, 2017.

461 Pajunoja, A., Lambe, A. T., Hakala, J., Rastak, N., Cummings, M. J., Brogan, J. F., Hao, L. Q., Paramonov, M., Hong,
462 J., Prisle, N. L., Malila, J., Romakkaniemi, S., Lehtinen, K. E. J., Laaksonen, A., Kulmala, M., Massoli, P., Onasch,
463 T. B., Donahue, N. M., Riipinen, I., Davidovits, P., Worsnop, D. R., Petaja, T., and Virtanen, A.: Adsorptive uptake
464 of water by semisolid secondary organic aerosols, *Geophys. Res. Lett.*, 42, 3063-3068,
465 <https://doi.org/10.1002/2015gl063142>, 2015.

466 Parsons, M. T., Mak, J., Lipetz, S. R., and Bertram, A. K.: Deliquescence of malonic, succinic, glutaric, and adipic acid
467 particles, *J. Geophys. Res.: Atmos.*, 109, D06212, <https://doi.org/10.1029/2003jd004075>, 2004.

468 Peng, C., Chan, M. N., and Chan, C. K.: The hygroscopic properties of dicarboxylic and multifunctional acids:
469 Measurements and UNIFAC predictions, *Environ. Sci. Technol.*, 35, 4495-4501, <https://doi.org/10.1021/es0107531>,
470 2001.

471 Peng, C., Jing, B., Guo, Y. C., Zhang, Y. H., and Ge, M. F.: Hygroscopic behavior of multicomponent aerosols involving
472 NaCl and dicarboxylic Acids, *J. Phys. Chem. A*, 120, 1029-1038, <https://doi.org/10.1021/acs.jpca.5b09373>, 2016.

473 Peng, C., Razafindrabinina, P. N., Malek, K. A., Chen, L. X. D., Wang, W. G., Huang, R. J., Zhang, Y. Q., Ding, X.,
474 Ge, M. F., Wang, X. M., Asa-Awuku, A. A., and Tang, M. J.: Interactions of organosulfates with water vapor under
475 sub- and supersaturated conditions, *Atmos. Chem. Phys.*, 21, 7135-7148, <https://doi.org/10.5194/acp-21-7135-2021>,
476 2021.

477 Peng, C., Chen, L., and Tang, M.: A database for deliquescence and efflorescence relative humidities of compounds with
478 atmospheric relevance, *Fundam. Res.*, 2, 578-587, <https://doi.org/10.1016/j.fmr.2021.11.021>, 2022.

479 Petters, M. D. and Kreidenweis, S. M.: A single parameter representation of hygroscopic growth and cloud condensation
480 nucleus activity, *Atmos. Chem. Phys.*, 7, 1961-1971, <https://doi.org/10.5194/acp-7-1961-2007>, 2007.

481 Petters, M. D., Kreidenweis, S. M., Prenni, A. J., Sullivan, R. C., Carrico, C. M., Koehler, K. A., and Ziemann, P. J.:
482 Role of molecular size in cloud droplet activation, *Geophys. Res. Lett.*, 36, <https://doi.org/10.1029/2009gl040131>,
483 2009.

484 Petters, S. S., Pagonis, D., Clafin, M. S., Levin, E. J. T., Petters, M. D., Ziemann, P. J., and Kreidenweis, S. M.:
485 Hygroscopicity of organic compounds as a function of carbon chain length and carboxyl, hydroperoxy, and carbonyl
486 functional groups, *J. Phys. Chem. A*, 121, 5164-5174, <https://doi.org/10.1021/acs.jpca.7b04114>, 2017.

487 Ray, K. K., Lee, H. D., Gutierrez, M. A., Jr., Chang, F. J., and Tivanski, A. V.: Correlating 3D morphology, phase state,
488 and viscoelastic properties of individual substrate-deposited particles, *Anal. Chem.*, 91, 7621-7630,
489 <https://doi.org/10.1021/acs.analchem.9b00333>, 2019.

490 Römpp, A., Winterhalter, R., and Moortgat, G. K.: Oxodicarboxylic acids in atmospheric aerosol particles, *Atmos.*
491 *Environ.*, 40, 6846-6862, <https://doi.org/10.1016/j.atmosenv.2006.05.053>, 2006.

492 Rose, D., Gunthe, S. S., Mikhailov, E., Frank, G. P., Dusek, U., Andreae, M. O., and Pöschl, U.: Calibration and
493 measurement uncertainties of a continuous-flow cloud condensation nuclei counter (DMT-CCNC): CCN activation
494 of ammonium sulfate and sodium chloride aerosol particles in theory and experiment, *Atmos. Chem. Phys.*, 8, 1153-
495 1179, <https://doi.org/10.5194/acp-8-1153-2008>, 2008.

496 Rose, D., Nowak, A., Achtert, P., Wiedensohler, A., Hu, M., Shao, M., Zhang, Y., Andreae, M. O., and Pöschl, U.:
497 Cloud condensation nuclei in polluted air and biomass burning smoke near the mega-city Guangzhou, China – Part
498 1: Size-resolved measurements and implications for the modeling of aerosol particle hygroscopicity and CCN
499 activity, *Atmos. Chem. Phys.*, 10, 3365-3383, <https://doi.org/10.5194/acp-10-3365-2010>, 2010.

500 Rosenfeld, D., Sherwood, S., Wood, R., and Donner, L.: Climate effects of aerosol-cloud interactions, *Science*, 343,
501 379-380, <https://doi.org/10.1126/science.1247490>, 2014.

502 Ruehl, C. R., Chuang, P. Y., and Nenes, A.: Aerosol hygroscopicity at high (99 to 100%) relative humidities, *Atmos.*
503 *Chem. Phys.*, 10, 1329-1344, <https://doi.org/10.5194/acp-10-1329-2010>, 2010.

504 Ruehl, C. R., Chuang, P. Y., Nenes, A., Cappa, C. D., Kolesar, K. R., and Goldstein, A. H.: Strong evidence of surface
505 tension reduction in microscopic aqueous droplets, *Geophys. Res. Lett.*, 39, L23801,
506 <https://doi.org/10.1029/2012gl053706>, 2012.

507 Ruehl, C. R. and Wilson, K. R.: Surface organic monolayers control the hygroscopic growth of submicrometer particles
508 at high relative humidity, *J. Phys. Chem. A*, 118, 3952-3966, <https://doi.org/10.1021/jp502844g>, 2014.

509 Ruehl, C. R., Davies, J. F., and Wilson, K. R.: An interfacial mechanism for cloud droplet formation on organic aerosols,
510 *Science*, 351, 1447-1450, <https://doi.org/10.1126/science.aad4889>, 2016.

511 Shiraiwa, M., Li, Y., Tsimpidi, A. P., Karydis, V. A., Berkemeier, T., Pandis, S. N., Lelieveld, J., Koop, T., and Pöschl,
512 U.: Global distribution of particle phase state in atmospheric secondary organic aerosols, *Nat. Commun.*, 8, 15002,
513 <https://doi.org/10.1038/ncomms15002>, 2017.

514 Sjögren, S., Gysel, M., Weingartner, E., Baltensperger, U., Cubison, M. J., Coe, H., Zardini, A. A., Marcolli, C., Krieger,
515 U. K., and Peter, T.: Hygroscopic growth and water uptake kinetics of two-phase aerosol particles consisting of
516 ammonium sulfate, adipic and humic acid mixtures, *J. Aerosol Sci.*, 38, 157-171,
517 <https://doi.org/10.1016/j.jaerosci.2006.11.005>, 2007.

518 Suda, S. R., Petters, M. D., Yeh, G. K., Strollo, C., Matsunaga, A., Faulhaber, A., Ziemann, P. J., Prenni, A. J., Carrico,
519 C. M., Sullivan, R. C., and Kreidenweis, S. M.: Influence of functional groups on organic aerosol cloud
520 condensation nucleus activity, *Environ. Sci. Technol.*, 48, 10182-10190, <https://doi.org/10.1021/es502147y>, 2014.

521 Vepsäläinen, S., Calderón, S. M., Malila, J., and Prisle, N. L.: Comparison of six approaches to predicting droplet
522 activation of surface active aerosol – Part 1: moderately surface active organics, *Atmos. Chem. Phys.*, 22, 2669-
523 2687, <https://doi.org/10.5194/acp-22-2669-2022>, 2022.

524 Wu, Z. J., Poulain, L., Henning, S., Dieckmann, K., Birmili, W., Merkel, M., van Pinxteren, D., Spindler, G., Müller, K.,
525 Stratmann, F., Herrmann, H., and Wiedensohler, A.: Relating particle hygroscopicity and CCN activity to chemical
526 composition during the HCCT-2010 field campaign, *Atmos. Chem. Phys.*, 13, 7983-7996,
527 <https://doi.org/10.5194/acp-13-7983-2013>, 2013.

528 Yazdanpanah, M. M., Hosseini, M., Pabba, S., Berry, S. M., Dobrokhoto, V. V., Safir, A., Keynton, R. S., and Cohn,
529 R. W.: Micro-wilhelmy and related liquid property measurements using constant-diameter nanoneedle-tipped
530 atomic force microscope probes, *Langmuir*, 24, 13753-13764, <https://doi.org/10.1021/la802820u>, 2008.

531 Zhang, C., Bu, L., Fan, F., Ma, N., Wang, Y., Yang, Y., Groß, J., Yan, J., and Wiedensohler, A.: Surfactant effect on the
532 hygroscopicity of aerosol particles at relative humidity ranging from 80% to 99.5%: Internally mixed adipic acid-
533 ammonium sulfate particles, *Atmos. Environ.*, 266, 118725–118736,
534 <https://doi.org/10.1016/j.atmosenv.2021.118725>, 2021.

535 Zhang, Y., Tao, J., Ma, N., Kuang, Y., Wang, Z., Cheng, P., Xu, W., Yang, W., Zhang, S., Xiong, C., Dong, W., Xie,
536 L., Sun, Y., Fu, P., Zhou, G., Cheng, Y., and Su, H.: Predicting cloud condensation nuclei number concentration

537 based on conventional measurements of aerosol properties in the North China Plain, *Sci. Total Environ.*, 719,
538 137473, <https://doi.org/10.1016/j.scitotenv.2020.137473>, 2020.

539 Zhao, D. F., Buchholz, A., Kortner, B., Schlag, P., Rubach, F., Fuchs, H., Kiendler-Scharr, A., Tillmann, R., Wahner,
540 A., Watne, Å. K., Hallquist, M., Flores, J. M., Rudich, Y., Kristensen, K., Hansen, A. M. K., Glasius, M., Kourtchev,
541 I., Kalberer, M., and Mentel, T. F.: Cloud condensation nuclei activity, droplet growth kinetics, and hygroscopicity
542 of biogenic and anthropogenic secondary organic aerosol (SOA), *Atmos. Chem. Phys.*, 16, 1105-1121,
543 <https://doi.org/10.5194/acp-16-1105-2016>, 2016.

544

545

546 **Table 1. Substances and their relevant properties investigated in this study.**

Compounds	Molar weight (g mol ⁻¹)	Density (g cm ⁻³)	Solubility (g L ⁻¹)	DRH (%RH)	Purity	Supplier
NaCl	58.44 ^a	2.16 ^a	360 ^b	73-77 ^c	<u>≥99.8%G</u> R	Sinopharm Chemical Reagent
AS	132.13 ^a	1.77 ^a	770 ^b	78-82 ^c	≥99%	Sigma Aldrich
MA	104.06 ^a	1.63 ^a	1400 ^b	65-76 ^c	≥99%	Sigma Aldrich
PhMA	180.16 ^a	1.40 ^a	131 ^a	NA	98%	Aladdin
SA	118.09 ^a	1.57 ^a	80 ^b	98 ^d	≥99%	Aladdin
PhSA	194.19 ^a	1.13 ^a	241 ^a	NA	98%	Macklin
AA	146.14 ^a	1.36 ^a	14.4 ^b	~100 ^e	<u>≥99.8%G</u> R	Sinopharm Chemical Reagent
PA	160.17 ^a	1.28 ^a	25 ^b	>90 ^c	99%	Macklin
OA	174.20 ^a	1.16 ^a	12 ^a	>90 ^c	99%	Aladdin

547 ^a <https://comptox.epa.gov/> (last access: 3rd August 2022). ^b <https://www.chemicalbook.com/> (last access: 3rd August 2022). ^c
548 Peng et al. (2022) and references therein. ^d Peng et al. (2001). ^e Parsons et al. (2004). DRH means deliquescence RH. GR
549 means guaranteed reagent. NA indicates no reported results are available.

550

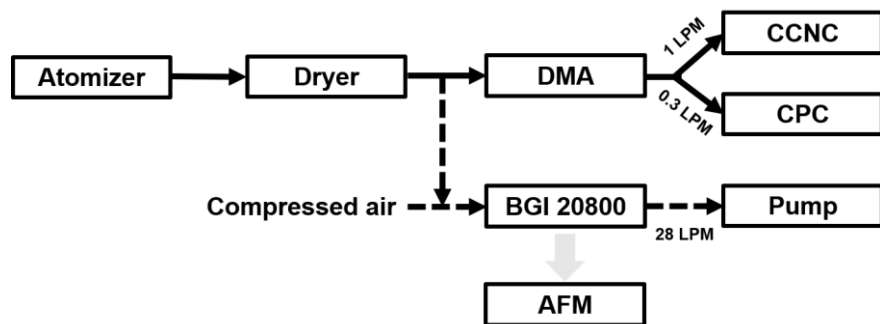
551 **Table 2. Summary of κ_{CCN} for single component particles.**

Chemicals	D_d (nm)	κ_{CCN}	Previous reported κ_{CCN}
		mean \pm standard deviation	
NaCl	50, 65, 76, 88, 100	1.325 \pm 0.038	1.28 ^a
AS	50, 65, 76, 88, 100	0.562 \pm 0.059	0.61 ^a
MA	50, 65, 76, 88, 100	0.240 \pm 0.036	0.227 ^a
PhMA	50, 65, 76, 88, 100	0.183 \pm 0.032	This study NA
SA	50, 65, 76, 88, 100	0.204 \pm 0.023	0.166-0.295 ^a
PhSA	50, 65, 76, 88, 100	0.145 \pm 0.017	This study NA
AA	140, 160, 180, 200	0.008 \pm 0.001	0.005-0.008 ^b
PA	65, 76, 88, 100	0.112 \pm 0.010	0.14 ^b
OA	200, 220, 240, 260	0.003 \pm 0.0002	0.001 ^b

552 ^a Petters et al., 2007; ^b Kuwata et al. (2013) and references therein. NA indicates no reported results are available.

553

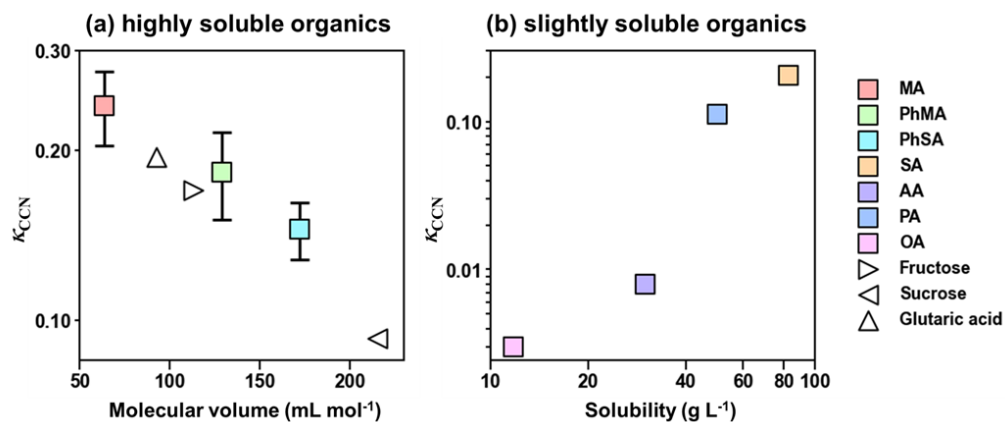
554



555

556 **Figure 1:** Schematic illustration of the instrumental set-up. The arrow indicates the flow direction. LPM means liter per minute.

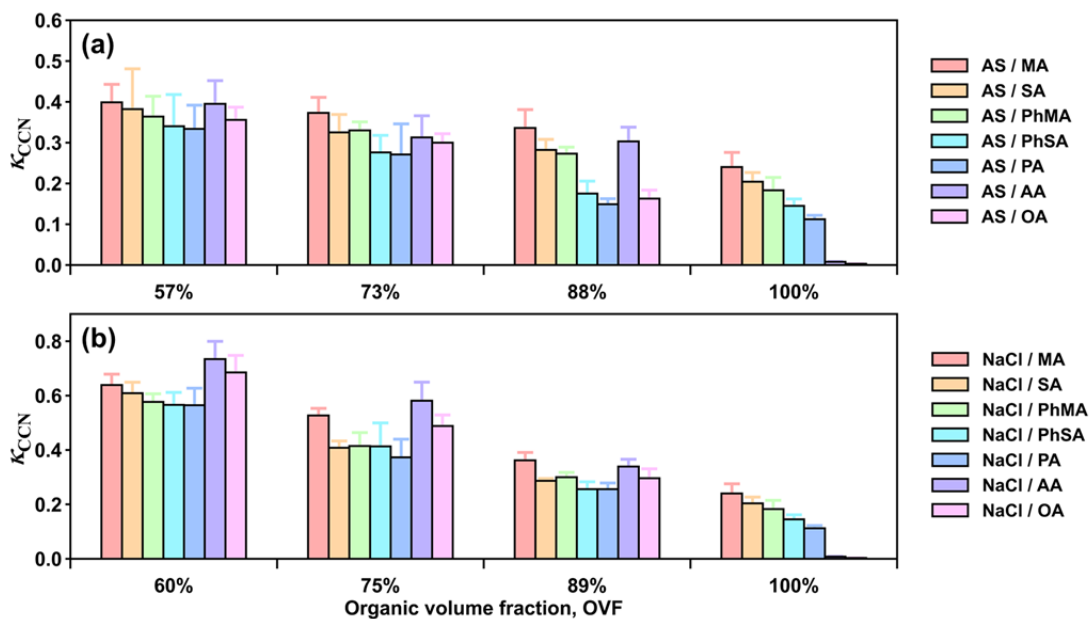
557



558

559 **Figure 2:** κ_{CCN} of organic compounds as a function of (a) molecular volume and (b) solubility. Solid squares represent κ_{CCN} results
560 in this study while hollow triangles were κ_{CCN} results obtained from Chan et al. (2008).

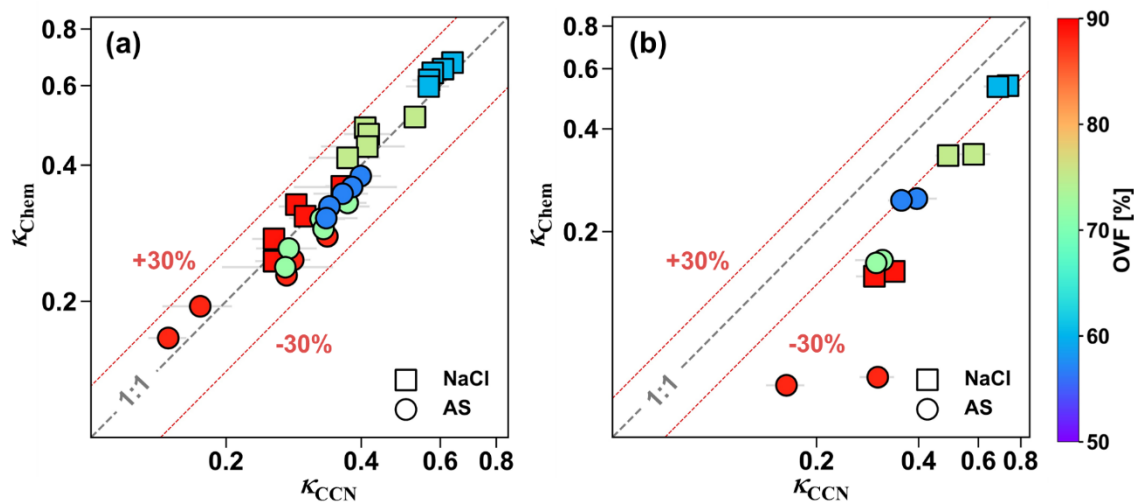
561



562

563 **Figure 3:** κ_{CCN} of (a) AS/dicarboxylic acid and (b) NaCl/dicarboxylic acid mixed particles with varied OVF.

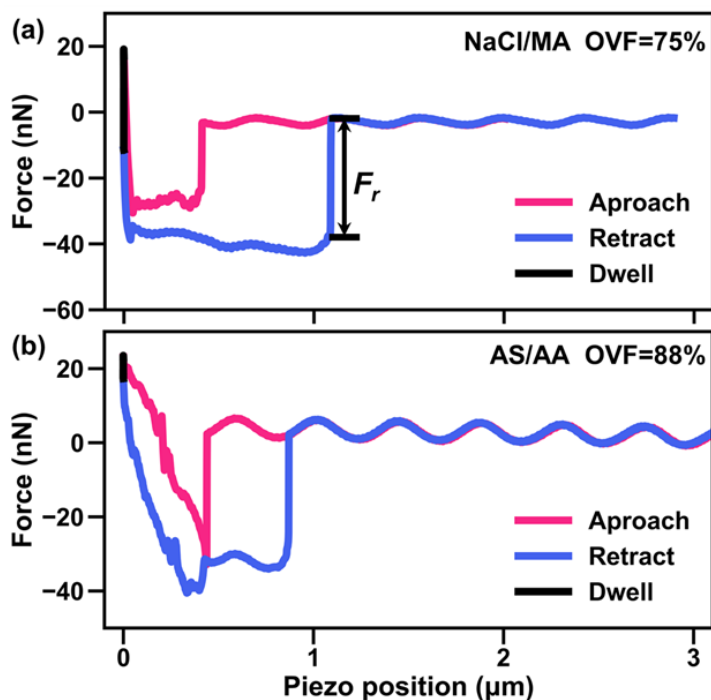
564



565

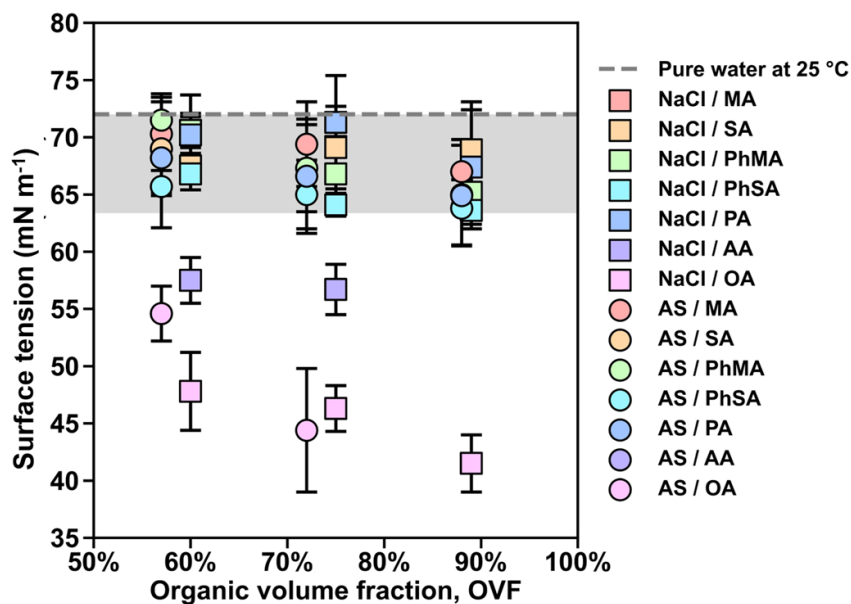
566 **Figure 4:** Comparison between κ_{CCN} and κ_{Chem} of (a) inorganic salt mixed with MA, PhMA, SA, PhSA and PA (b) inorganic salt
 567 mixed with AA and OA. Square represents NaCl containing particles and circle represents AS containing particles. Color bar
 568 indicates OVF.

569



570

571 Figure 5: AFM force plots of (a) NaCl/MA system with 75% OVF and (b) AS/AA system with 88% OVF. F_r is the retention force to
 572 break the meniscus by the tip of AFM probe.



573

574 Figure 6: Measured surface tension values of inorganic salt/dicarboxylic acid particles under RH over 99.5%. Gray area covers the
 575 surface tension reductions below 12% comparing with pure water (72 mN m^{-1}).